Published in final edited form as:

Nature. 2010 June 10; 465(7299): 793–797. doi:10.1038/nature09135.

Quiescent hematopoietic stem cells are activated by IFNγ in response to chronic infection

Megan T. Baldridge[1,*], **Katherine Y. King**[2,*], **Nathan C. Boles**[3], **David C. Weksberg**[1], and **Margaret A. Goodell**[1,2,3]

[1]Department of Molecular and Human Genetics, Baylor College of Medicine, Houston, Texas, 77030, USA

[2]Department of Pediatrics, Section of Infectious Diseases, Baylor College of Medicine, Houston, Texas, 77030, USA

[3]Interdepartmental Program in Cell and Molecular Biology, Baylor College of Medicine, Houston, Texas, 77030, USA

Summary

Lymphocytes and neutrophils are rapidly depleted by systemic infection1. Progenitor cells of the hematopoietic system, such as common myeloid progenitors (CMPs) and common lymphoid progenitors (CLPs), increase the production of immune cells to restore and maintain homeostasis during chronic infection, but the contribution of hematopoietic stem cells (HSCs) to this process is largely unknown2. Using an *in vivo* mouse model of *Mycobacterium avium* infection, we show that an increased proportion of long-term repopulating HSCs (LT-HSCs) proliferate during *M. avium* infection, and that this response requires interferon-gamma (IFNγ) but not interferon-alpha (IFNα) signaling. Thus, the hematopoietic response to chronic bacterial infection involves the activation not only of intermediate blood progenitors but of LT-HSCs as well. IFNγ is sufficient to promote LT-HSC proliferation *in vivo*; furthermore, HSCs from mice deficient in IFNγ have a lower proliferative rate, indicating that baseline IFNγ tone regulates HSC activity. These findings are the first to implicate IFNγ both as a regulator of HSCs during homeostasis and under conditions of infectious stress. Our studies contribute to a deeper understanding of hematologic responses in patients with chronic infections such as HIV/AIDS or tuberculosis3-5.

As the precursors of all blood cells, HSCs remain dormant during most of the life of an organism, entering the cell cycle only when necessary to generate differentiated progeny6, 7.

Corresponding author: Margaret A. Goodell One Baylor Plaza, N1030 Houston, TX 77030 Phone: 713-798-1265 Fax: 713-798-1230 goodell@bcm.edu.

*These authors contributed equally to this work.

Author contributions M.T.B. and K.Y.K. designed experiments, performed flow cytometry, transplants, and quantitative real-time PCR analysis, and analyzed data. K.Y.K. performed immunohistochemistry. N.C.B. performed flow cytometry and cytokine analysis. D.C.W. assisted with study design. M.T.B., K.Y.K., and M.A.G. wrote the manuscript. All authors discussed results and commented on the manuscript.

Supplementary Information is linked to the online version of the paper at www.nature.com/nature.

Author information Reprints and permissions information is available at npg.nature.com/reprintsandpermissions.

Maintenance of the blood and immune systems imposes different stresses on HSCs, ranging from the routine demands of cellular senescence to the extreme stress of acute bleeding, when the production of peripheral blood cells must be increased many-fold8. The signals that trigger HSC activation remain largely unknown. Because infection is a common natural stressor that leads to the consumption of peripheral immune cells, we sought to determine whether replenishment of immune cells during chronic infection requires only immediate myeloid and lymphoid precursors or if activation of HSCs is also required9, 10. Further, we investigated the role of the interferon family of inflammatory cytokines in influencing HSC activation.

Earlier studies by our group and others have noted an increase in the absolute and relative number of primitive progenitor cells of the bone marrow in response to chronic infection11-13. These results were obtained by phenotypically tracking cells that expressed the stem cell markers c-Kit and Sca-1 while lacking the canonical markers of lineage differentiation (so-called KSL cells). Thus far, however, neither the mechanism nor the functional consequence of this change has been fully explored. For instance, what signaling molecules affect HSCs during infection, and do they promote a proliferative response? To address these questions, we chose a mouse model of *Mycobacterium avium* infection, which affords an example of chronic systemic mycobacterial diseases, including tuberculosis14, and enables us to study HSCs without disrupting their natural microenvironment.

When injected intravenously with *M. avium*, wild-type mice were systemically infected with large numbers of bacteria at 4 weeks postinjection and had larger spleens, consistent with sequestration of bacteria and lymphoid cells in the spleen (Supplementary Fig. 1)15. Despite infection with *M. avium*, the absolute numbers of lymphocytes, neutrophils, monocytes, eosinophils and basophils in peripheral blood remained stable; the only significant changes in blood composition were a decrease in platelet number at 2 weeks postinfection (Supplementary Fig. 2A) and a relative decrease of B cells with an associated increase of $CD4^+$ T-cells and granulocytes at 4 weeks postinfection (Supplementary Fig. 2B). The bone marrow showed a loss of granulocyte-monocyte progenitors, common myeloid progenitors, and macrophage-erythroid progenitors from 2 to 4 weeks postinfection with a concomitant increase in common lymphoid progenitors (Supplementary Fig. 3). These changes are consistent with mobilization of a T-cell-mediated immune response, characteristic of ongoing mycobacterial disease15.

Given the observed changes in intermediate progenitor populations in *M. avium*-infected mice, we asked whether earlier progenitors might be activated to expand during chronic infection. To assess the response of early hematopoietic progenitors to *M. avium* infection, we determined the absolute numbers of short-term repopulating HSCs (ST-HSCs: KSL, $CD34^+$, $Flk2^-$) and multipotent progenitors (MPPs: KSL, $CD34^+$, $Flk2^+$; gating shown in Supplementary Figure 4) in mice observed over 4 weeks after infection. There was a sharp increase ($P<0.001$) in ST-HSCs (Fig. 1A), cells that are highly proliferative and can maintain pluripotency for several weeks16. These findings suggest that compensatory expansion of these progenitors maintains blood cell homeostasis over the course of a chronic *M. avium* infection.

To assess the effect of mycobacterial infection on the most primitive progenitor populations of the bone marrow, we analyzed the long-term repopulating HSCs (LT-HSCs). LT-HSCs were phenotypically defined by surface markers (KSL, CD34−, Flk2− or KSL, CD150+)16, 17 or a combination of vital dye staining and surface markers (side population, or SP, along with KLS – SP^{KLS})18. Where experimentally possible, we conducted experiments using multiple phenotypic definitions of LT-HSCs in order to verify that our observations were not due to stress-induced alterations in marker expression. After conducting *M. avium* infection in wild type animals for 4 weeks, we found that the absolute numbers of LT-HSC were increased marginally (Fig 1A, KSL Flk2− CD34−) or not at all (SP^{KLS}, Fig. 1B).

The expansion in ST-HSCs with minimal increase in LT-HSC number suggested that the LT-HSCs may be proliferating to meet the increased demand for their immediate downstream progeny, namely ST-HSC and MPP. To examine this possibility, we determined the proliferative status of the LT-HSCs during *M. avium* infection by measuring their relative incorporation of 5-bromo-2′-deoxyuridine (BrdU)19. The results demonstrated an increased percentage of proliferating LT-HSCs (SP^{KLS}) in the bone marrow of infected mice compared with the level prior to infection (Fig. 1C). We also confirmed these findings by Hoechst and Pyronin Y staining to assess the cell cycle status of HSCs from uninfected and infected animals19. The *M. avium* infected mice had a significantly lower percentage of quiescent (G_0) HSCs compared to uninfected mice (Supplementary Fig. 5). Thus, *M. avium* infection appears to stimulate an increase in the proliferative fraction of primitive LT-HSCs, along with a substantial increase in the numbers of early committed progenitors.

If the proliferative fraction of LT-HSCs from infected mice is indeed increased, such cells may be expected to lose some regenerative function and to engraft less readily than HSCs from uninfected mice, as has been shown for proliferating HSCs20. To test this, we transplanted 500 LT-HSCs from naïve or *M. avium*-infected mice into irradiated wild-type CD45.1 recipients together with a radioprotective dose of 2×10^6 recipient-type CD45.1 whole bone marrow (WBM) cells. At short time points after transplantation, the LT-HSCs from infected mice showed impaired engraftment compared with those from uninfected mice, consistent with their increased proliferative status (Fig. 1D). Of note, few if any *M. avium* bacteria could be isolated from the donor whole bone marrow, and no bacteria were isolated from the spleens of recipient mice 20 weeks after transplantation, indicating that infectious particles were not transmitted with the cell transplants. We conclude from these data that chronic mycobacterial infection induces proliferation of HSCs, with functional consequences that cannot be attributed to infection of the stem cells themselves.

Given the finding that LT-HSCs are more highly proliferative during chronic *M. avium* infection without a large change in their absolute number in the bone marrow, we wondered if the cells were being increasingly mobilized to leave the bone marrow during infection. To assess this possibility, we measured the number of LT-HSCs detectable in the spleen following infection. Infection with *M. avium* led to a striking increase in the number of phenotypic-HSCs in the spleen (Fig. 1E), suggesting mobilization of some of these cells during infection.

Soon after infectious stress is imposed, hematopoietic progenitors begin to proliferate in order to restore homeostasis, yet the signaling pathways involved in this response are largely unknown10, 21. Because IFNγ is strongly upregulated during *M. avium* infection15, 22, we focused our attention on the interferons23. We hypothesized that IFNγ is responsible for the proliferative response of HSCs during *M. avium* infection. To confirm that *M. avium* infection in mice leads to an increase of IFNγ in bone marrow, where HSCs reside, we collected bone marrow supernatants from naive and infected mice at 4 weeks postinfection. Consistent with previous findings in serum15, 22, analysis of the samples by a cytokine bead array method indicated strong upregulation of IFNγ in the bone marrow of mice infected with *M. avium* (Fig. 2A).

Because many different cytokines are active during periods of infectious stress, we sought to determine if IFNγ is necessary to influence the behavior of HSCs. We predicted that interference with IFNγ signaling would abrogate the HSC response to *M. avium* infection. Therefore, we analyzed the HSCs in bone marrow samples from naïve and infected mice lacking essential components of the IFNγ-signaling pathway, including mice lacking the interferon-gamma receptor 1 (*Ifngr1*) gene or the *Stat1* gene encoding the downstream signal transducer for IFNGR1. Animals lacking functional *Ifngr1* or *Stat1* showed an impaired proliferative response of the LT-HSC compartment as measured by BrdU incorporation (Fig. 2B). However, proliferative activation of LT-HSCs occurred normally in mice lacking functional interferon-alpha receptor 1 (IFNAR1), suggesting that IFNα signaling is not required for this response (Fig. 2B). Similarly, the modest numerical increase observed in phenotypically-defined HSC in response to infection was abrogated in IFNγ signaling mutants (Fig. 2C). Furthermore, when the same infection was carried out in mice lacking the IFNα receptor (IFNAR1), the HSC response was intact. These results collectively support an essential role for IFNγ but not IFNα in the proliferative activation of HSCs in response to *in vivo* infection by *M. avium*.

We next turned our attention to determine whether LT-HSCs respond directly to IFNγ stimulation, and whether IFNγ alone is sufficient to induce these effects. Previous work from our group indicated that LT-HSCs express the IFNγ receptor subunit 1 (IFNGR1), allowing them to respond directly to IFNγ signaling24. We confirmed that *Ifngr1* is expressed by HSCs using real-time quantitative PCR analysis (Fig. 3A). Indeed, the amount of *Ifngr1* mRNA in HSCs was significantly higher than that in T-cells, B-cells, and granulocytes, all known to express high levels of this receptor25. To assess the function of the IFNGR1 receptor on LT-HSCs, we treated purified LT-HSCs with IFNγ *in vitro* and examined them for changes in mRNA levels of a known IFN-inducible gene, *Irgm1*26. We found that *Irgm1* expression is upregulated in response to IFNγ exposure *in vitro*, and that this response is abrogated in *Ifngr1*-deficient and *Stat1*-deficient HSCs (Fig. 3B). These results were confirmed by an increase in IRGM1 protein levels in IFNγ-treated versus untreated mouse HSCs stained with anti-IRGM1 antibody and FITC-conjugated secondary antibody (green) (Fig. 3C). Furthermore, other interferon-regulated genes including *Stat1*, *Irf1*, and *Irf9* were upregulated in HSCs after *in vitro* IFNγ exposure when measured by real-time quantitative PCR, indicating that typical IFNγ-signaling pathways were activated in the purified cells (Supplementary Fig. 6)27.

The above findings suggested that one could trigger HSC proliferation with purified mouse recombinant IFNγ (rIFNγ) alone. We measured HSC proliferation in response to induction by rIFNγ *in vitro*, and we found that primitive hematopoietic cells are significantly more proliferative after rIFNγ treatment (Fig. 3D) with no increase in apoptosis (Supplementary Figure 7). This rapid *in vitro* response suggests the IFNγ–dependent effects on the HSC are independent of other physiologic changes in the bone marrow.

In order to determine if these effects also occurred *in vivo*, we injected wild-type mice intravenously with 10 mg of rIFNγ, conducted BrdU injection 12 hours later, and analyzed the proliferative status of the HSC after 12 additional hours. Analysis of BrdU incorporation into LT-HSCs from treated and untreated mice showed a significant increase in the percentage of proliferating stem cells in response to IFNγ treatment (Fig. 4A). Transplants using WBM from rIFNγ-treated mice showed modest impairment in the functional reconstitution capacity of rIFNγ-exposed cells compared to WBM from untreated mice (Fig. 4B). Finally, increased mobilization of primitive hematopoietic cells to the spleen could also be detected following *in vivo* treatment with purified IFNγ (Fig. 4C). Together, these experiments demonstrate that IFNγ directly affects HSCs and that exposure to IFNγ alone is sufficient to induce their proliferation and mobilization.

Given our findings that IFNγ is both necessary and sufficient for HSC proliferation and mobilization during *M. avium* infection, we hypothesized that mice lacking the IFNγ cytokine may show alterations in their HSC compartments. When we investigated the bone marrow of IFNγ-deficient animals, we found that LT-HSCs were less proliferative *even in the absence of infection* (Fig. 5A), but the total number of phenotypically-defined LT-HSCs was not different between wild type and IFNγ-deficient mice (Supplementary Fig. 8). We tested the functional capacity of the *Ifng*$^{-/-}$ HSCs in noncompetitive transplants (2×10^6 donor whole bone marrow cells) and competitive transplants (2×10^6 donor whole bone marrow cells competing against 2×10^6 CD45.1 whole bone marrow cells). Consistent with their decreased baseline proliferative status, HSCs from IFNγ-deficient mice showed improved engraftment compared to wild-type HSCs in competitive transplant assays (Fig. 5B). Since the phenotypic HSC number appears to be the same in WT and IFNγ-deficient mice, the improved engraftment is likely to result from the higher level of quiescence, as this property is inextricably linked to engraftment potential and HSC quality7,20. These results suggest that IFNγ stimulates HSCs even in the steady state, and that baseline IFNγ tone may influence HSC turnover and quality during normal homeostasis.

This work provides evidence that long-term repopulating HSCs can respond directly to IFNγ stimulation in the context of a chronic infection. The LT-HSC numbers, defined phenotypically and functionally, remain relatively constant, but a larger proportion are in cycle. This activation is accompanied by a substantial increase in the number of immediate downstream progenitors and maintenance of stable numbers of differentiated peripheral blood cells. These findings suggest that IFNγ promotes proliferation of the HSC to feed the generation of the immediate downstream progenitors, which in turn replenish immune effector cells during an ongoing infectious process. A recent report found that acute treatment of mice with purified IFNα or the IFNα-inducing agent poly(I:C) leads to cell-autonomous HSC proliferation, which was absent in *Ifnar*$^{-/-}$ and *Stat1*$^{-/-}$ mice28. In that

study, HSCs lacking the IFNα receptor were still able to respond to IFNα treatment when mixed with a high percentage of wild-type cells, indicating that other signaling pathways can compensate for the lack of IFNα in HSC activation. Our study raises the intriguing possibility that IFNα and IFNγ can coordinately regulate HSC activation in the context of an infection, most likely in a pathogen-specific manner.

A working model of IFNγ-mediated stimulation of quiescent HSCs, with increased proliferation and mobilization during a chronic bacterial infection, is shown in Supplementary Figure 9. In contrast to the very low proliferative/differentiative activity of dormant HSCs associated with low levels of IFNγ under normal physiological conditions (top panel), our model predicts that bacterial infection detected by sentinel immune cells stimulates the increased release of IFNγ, which then travels through the bloodstream to activate HSCs in the bone marrow, leading to expansion and mobilization of the immune progenitor pool (lower panel). While cell division is required for HSC to generate large numbers of downstream progenitors to replenish a stressed hematopoietic system, sustained HSC proliferation has repeatedly been shown to compromise long-term HSC quality and bone marrow transplant capacity 7, 20. We show here that increased proliferation in the context of chronic infection or direct exposure to IFNγ can lead to at least transient impairment of HSC function. We speculate that in some contexts, chronic infection or inflammation can ultimately lead to more substantive deficits in the ability of the LT-HSC compartment to sustain blood production. Deepened understanding of the molecular mechanisms used by HSCs to respond to chronic inflammatory stimuli could lead to improved clinical insight into the pathophysiology of bone marrow suppression in patients with chronic infections such as tuberculosis and HIV/AIDS3, 4.

Methods Summary

Mice

Mice were 6 to 12 weeks of age, including wild-type C57Bl/6 (CD45.2), wild-type C57Bl/6.SJL (CD45.1), C57Bl/6 *Ifng*$^{-/-}$, and C57Bl/6 *Ifngr1*$^{-/-}$ mice from Jackson Laboratories (Bar Harbor, ME), C57Bl/6 *Stat*$^{-/-}$ mice from David Levy (NYU), and C57Bl/6 *Ifnar1*$^{-/-}$ mice from Christian Schindler (Columbia University).

Mycobacterial infection and interferon treatment

Mice were infected intravenously (IV) with 2×10^6 colony-forming units of *M. avium* as described30. For IFNγ treatments, HSCs were incubated with 100 ng/mL rIFNgR&D [Minneapolis, MN]) at 37°C for 1 hour before real-time PCR, 12 hours for BrdU analysis, and 18 hours before immunofluorescence. For *in vivo* treatments, each mouse was injected with 10 μg IFNγ IV.

Flow cytometry and BrdU analysis

Peripheral blood was analyzed with a Hemavet 950. MoFlo, LSRII, and FACS-Scan instruments were used for flow cytometric analysis and sorting. Progenitor and HSC populations were identified, and HSC BrdU analysis performed as described21.

Immunohistochemistry

HSCs were stained with anti-IRGM1 antibody (1:100 v/v) (Santa Cruz sc-11077) by standard methods. Images were gathered with a DeltaVision restoration microscope and Softworx© imaging software.

Quantitative real-time PCR and cytokine detection

Irgm1, Ifngr1, Stat1, Irf1, and *Irf9* probes were used with Taqman PCR Mastermix and a 7900HT Fast Real-Time PCR system. Triplicate samples were normalized to internal 18S controls (Applied Biosystems [Foster City, CA]).

IFNγ levels were determined using an IFNγ BD cytokine bead array and BD FacsArray plate reader. Protein content of bone marrow supernatant was quantified using a NanoDrop spectrophotometer (NanoDrop Technologies [Oxfordshire, U.K.]).

Transplants

For bone marrow transplants, a mixture of test CD45.2 WBM and wild-type CD45.1 WBM was injected IV into CD45.1 mice that were irradiated with a split dose of 10.5 Gy, as described13. Engraftment was assessed at 4-week intervals.

Statistics

Mean values ± SEM are shown. Student's t-test or ANOVA was used for comparisons (GraphPad Prism Version 5.0). * $P<0.05$, ** $P<0.01$, *** $P<0.001$.

Methods

Mice

Wild-type C57Bl/6 (CD45.2) and C57Bl/6.SJL (CD45.1) mice 6-12 weeks of age were used. C57Bl/6 *Ifng*-/- (Stock #2287) and *Ifngr1*-/- (Stock #3288) mice were obtained from Jackson Laboratories (Bar Harbor, ME). C57Bl/6 *Stat1*-/- mice were obtained from David Levy (NYU)31, and C57Bl/6 *Ifnar1*-/- mice were obtained from Christian Schindler (Columbia University)32. All mouse strains were maintained at an AALAC-accredited, specific-pathogen-free animal facility. All mice were between 6 and 12 weeks of age at the time of experimentation.

Mycobacterial infection and interferon treatment

Mice were infected intravenously (IV) with 2×10^6 colony-forming units of *Mycobacterium avium* (SmT 2151) in a volume of 200 μL saline by IV retroorbital injection as previously described33. Unless otherwise noted, *M. avium* infections were allowed to proceed for 4 weeks prior to analysis of the infected animals. Bacterial colony counts were confirmed by growth of bacterial or whole bone marrow suspensions on Middlebrook 7H10 agar (Difco) plates at 37°C with 5% CO2 for 10-14 days. Experiments were repeated a minimum of two times with a minimum of 3 animals per cohort.

For *in vitro* IFNγ treatments, WBM was incubated in StemPro media (Invitrogen [Carlsbad, CA]) supplemented with thrombopoietin and stem cell factor as well as 100 ng/mL rIFNγ

(R&D [Minneapolis, MN]) at 37°C prior to further analysis or sorting. Incubation times were for 1 hour before real-time PCR, 12 hours for BrdU analysis, and 18 hours before immunofluorescence. For *in vivo* IFNγ treatments, mice were injected by retroorbital IV injection with 10 μg IFNγ in a volume of 200 μL saline 24 hours prior to analysis.

Flow cytometry and BrdU analysis

Peripheral blood was analyzed with a Hemavet 950. MoFlo, LSRII, and FACS-Scan instruments were used for flow cytometric analysis and cell sorting. Progenitor and HSC populations were identified and purified as previously described34,35. Briefly, antibodies against the following lineage markers were used: Mac-1, CD4, CD8, Ter119, Gr-1, and B220 (eBiosciences [San Diego, CA]). For immunophenotypic characterization of LT-HSCs, whole bone marrow was stained with antibodies against lineage markers, cKit, Sca-1, and CD150. For Figure 2A, LT-HSCs are defined as cKit+, Sca-1+, Lineage-(KSL), Flk2−, CD34−. For spleen, LT-HSCs are defined as KSL CD150+. Multipotent progenitors were identified by staining for the following markers: KSL, CD34+, Flk2+; for ST-HSC, cKit+, Lin−, CD34+, Flk2+; for CMPs, cKit+, Lin−, CD34+, FCgr−, Il7ra−; for GMPs, cKit+, Lin −, CD34+, FCgr+, Il7ra−; for MEPs, cKit+, Lin−, CD34−, FCgr−, IL7ra−; and for CLPs, cKit+, Lin−, Il7ra+4. For Hoechst dye efflux, whole bone marrow was incubated with Hoechst 33342 dye for 90 minutes at 37°C prior to staining with antibodies against cell surface markers. Pyronin Y/Hoechst analysis and Annexin V/PI staining were performed as previously described34,36.

HSC BrdU analysis was performed as described with 1 mg BrdU per 6g of mouse weight injected intraperitoneally 12 hours or 3 days prior to analysis21. For the 3-day experiment, BrdU (Sigma) was also added at 1 mg/mL to the drinking water. For *in vitro* analysis, BrdU was added at a concentration of 10 μM to the media for 12 hours. HSCs were sorted into a tube containing 300,000-500,000 carrier B220+ cells prior to fixation, DNase treatment, and cell staining using the BrdU FITC Flow Kit (BD PharMingen). Flow cytometric analysis of cells was conducted using a FacScan flow cytometer. Analysis of all flow cytometry data was conducted using FlowJo (Treestar, [Ashland, OR]). Data reflect at least two independent experiments, each conducted in triplicate.

Immunohistochemistry

HSCs were fixed with 4% paraformaldehyde, permeabilized with 10% Triton-X 100 for 30 minutes and blocked with 10% goat serum for 1 hour (Sigma [St. Louis,MO]). Slides were stained with anti-IRGM1 antibody (Santa Cruz sc-11077) at 1:100 v/v concentration at 4°C overnight and counterstained with rabbit anti-goat 488 secondary antibody at 1:400 v/v concentration for 30 minutes at room temperature. Cells were visualized with a DeltaVision restoration microscope with 100x objective and images processed with Softworx© imaging software.

Quantitative real-time PCR and cytokine detection

RNA was prepared using a column purification system (RNaqueous, Ambion) and cDNA was made using random hexamers and Superscript II reverse transcriptase (Invitrogen). *Irgm1*, *Ifngr1*, *Stat1*, *Irf1*, and *Irf9* probes (Applied Biosystems [Foster City, CA]) were used

with Taqman PCR Mastermix and a 7900HT Fast Real-Time PCR system. Samples run in triplicate were normalized to internal 18S controls (Applied Biosystems [Foster City, CA]).

IFNγ levels were detected with a mouse IFNγ BD cytokine bead array and BD FacsArray plate reader. Bone marrow supernatant was isolated from mouse tibias and femurs by suspending the bones in P200 pipette tips trimmed to fit into 1.5-mL Eppendorf tubes containing 10 mL PBS and centrifuging them at 3000 rpm for 8 minutes. The discharged marrow was pooled and centrifuged again, then the clear supernatant isolated and total protein quantified with a NanoDrop spectrophotometer (NanoDrop Technologies [Oxfordshire, U.K.]).

Transplants

For assessment of functional self-renewal capacity, whole bone marrow from donor CD45.2 animals was admixed with an equal radioprotective dose of whole bone marrow from a wild type, uninfected CD45.1 mouse. The serum-free suspension was injected IV into CD45.1 mice that had been lethally irradiated with a split dose of 10.5 Gy, as previously described13. For competitive transplants, 2×10^6 CD45.2 donor WBM cells were mixed with 2×10^6 wild type CD45.1 competitor WBM cells prior to injection into CD45.1 recipients. For noncompetitive transplants, only 2×10^6 CD45.2 donor WBM cells were used. Bone marrow transplantation of purified HSCs was done using 500 LT-HSCs (SP^{KLS}) isolated from CD45.2 mice mixed with a radioprotective dose of 2×10^5 wild-type CD45.1 competitor WBM cells prior to injection into CD45.1 recipients. A minimum of 2 donor mice and 5 transplanted recipient mice were used for every cohort. Engraftment was assessed at 4-week intervals by determining the relative percentage of peripheral WBCs carrying the CD45.1 versus CD45.2 marker.

Statistics

Mean values ± SEM are shown. Student's t-test or ANOVA was used for comparisons (GraphPad Prism Version 5.0). * $P<0.05$, ** $P<0.01$, *** $P<0.001$.

Supplementary Material

Refer to Web version on PubMed Central for supplementary material.

Acknowledgements

We thank Carl Feng and Alan Sher for providing *Mycobacterium avium*. We also thank David Levy and Christian Schindler for providing us with *Stat1* and *Ifnar1* knock-out mice. We are grateful to Grant Challen for providing information about IFNgR1, to Yayun Zheng and Shihua Wu for technical assistance, and to John Gilbert for critical reading of the manuscript. M.T.B. is supported by the NIDDK institute of the NIH, and K.Y.K. was supported by the Adeline B. Landa Fellowship of the Texas Children's Hospital Auxiliary and the Simmons Foundation Collaborative Research Fund. This work was supported by the NIDDK, NHLBI, and NIBIB institutes of the NIH. The content is solely the responsibility of the authors and does not necessarily represent the official views of the National Institutes of Health.

References

1. Hawkins C, Collignon P, Adams D, Bowden F, Cook M. Profound lymphopenia and bacteraemia. Intern Med J. 2006; 36:385–388. [PubMed: 16732866]

2. Marleau AM, Sarvetnick N. T cell homeostasis in tolerance and immunity. J Leukoc Biol. 2005; 78:575–84. [PubMed: 15894586]

3. Singh KJ, et al. Significance of haematological manifestations in patients with tuberculosis. The Journal of the Association of Physicians of India. 2001; 49:788, 790–4. [PubMed: 11837465]

4. Sundell IB, Koka PS. Chimeric SCID-hu Model as a Human Hematopoietic Stem Cell Host That Recapitulates the Effects of HIV-1 on Bone Marrow Progenitors in Infected Patients. Journal of stem cells. 2006; 1:283–300. [PubMed: 19030112]

5. Klautau GB, Kuschnaroff TM. Clinical forms and outcome of tuberculosis in HIV-infected patients in a tertiary hospital in São Paulo - Brazil. Braz J Infect Dis. 2005; 9:464–78. [PubMed: 16410941]

6. Venezia T, et al. Molecular Signatures of Proliferation and Quiescence in Hematopoietic Stem Cells. Plos Biol. 2004; 2:e301. [PubMed: 15459755]

7. Wilson A, et al. Hematopoietic stem cells reversibly switch from dormancy to self-renewal during homeostasis and repair. Cell. 2008; 135:1118–29. [PubMed: 19062086]

8. Cheshier S, Prohaska S, Weissman I. The Effect of Bleeding on Hematopoietic Stem Cell Cycling and Self-Renewal. Stem Cells and Development. 2007; 16:707–718. [PubMed: 17999593]

9. Shahbazian L, et al. Escherichia coli pneumonia enhances granulopoiesis and the mobilization of myeloid progenitor cells into the systemic circulation. Critical Care Medicine. 2004; 32:1740–1746. [PubMed: 15286552]

10. Zhang P, et al. The lineage-c-Kit+Sca-1+ cell response to Escherichia coli bacteremia in Balb/c mice. Stem Cells. 2008; 26:1778–86. [PubMed: 18483422]

11. Singh P, et al. Vaccinia Virus Infection Modulates the Hematopoietic Cell Compartments in the Bone Marrow. Stem Cells. 2008; 26:1009–1016. [PubMed: 18258722]

12. Murray PJ, Young RA, Daley GQ. Hematopoietic remodeling in interferon-gamma-deficient mice infected with mycobacteria. Blood. 1998; 91:2914–24. [PubMed: 9531602]

13. Feng C. The p47 GTPase Lrg-47 (Irgm1) Links Host Defense and Hematopoietic Stem Cell Proliferation. Cell Stem Cell. 2008; 2:83–89. [PubMed: 18371424]

14. Appelberg R. Pathogenesis of Mycobacterium avium infection: typical responses to an atypical mycobacterium? Immunol Res. 2006; 35:179–90. [PubMed: 17172645]

15. Saunders BM, Dane A, Briscoe H, Britton WJ. Characterization of immune responses during infection with Mycobacterium avium strains 100, 101 and the recently sequenced 104. Immunol Cell Biol. 2002; 80:544–9. [PubMed: 12406388]

16. Christensen JL, Weissman IL. Flk-2 is a marker in hematopoietic stem cell differentiation: a simple method to isolate long-term stem cells. Proc Natl Acad Sci USA. 2001; 98:14541–6. [PubMed: 11724967]

17. Kiel MJ, Yilmaz OH, Iwashita T, Terhorst C, Morrison SJ. SLAM family receptors distinguish hematopoietic stem and progenitor cells and reveal endothelial niches for stem cells. Cell. 2005; 121:1109–21. [PubMed: 15989959]

18. Camargo FD, Chambers SM, Drew E, McNagny KM, Goodell MA. Hematopoietic stem cells do not engraft with absolute efficiencies. Blood. 2006; 107:501–7. [PubMed: 16204316]

19. Challen GA, Boles N, Lin KK, Goodell M. Mouse hematopoietic stem cell identification and analysis. Cytometry A. 2009; 75:14–24. [PubMed: 19023891]

20. Passegue E, Wagers AJ, Giuriato S, Anderson WC, Weissman IL. Global analysis of proliferation and cell cycle gene expression in the regulation of hematopoietic stem and progenitor cell fates. J Exp Med. 2005; 202:1599–611. [PubMed: 16330818]

21. Ezoe S, Matsumura I, Satoh Y, Tanaka H, Kanakura Y. Cell cycle regulation in hematopoietic stem/progenitor cells. Cell Cycle. 2004; 3:314–8. [PubMed: 14726670]

22. Flórido M, et al. Gamma interferon-induced T-cell loss in virulent Mycobacterium avium infection. Infection and Immunity. 2005; 73:3577–86. [PubMed: 15908387]

23. Platanias L. Mechanisms of type-I- and type-II-interferon-mediated signalling. Nat Rev Immunol. 2005; 5:375–386. [PubMed: 15864272]

24. Chambers S, et al. Aging Hematopoietic Stem Cells Decline in Function and Exhibit Epigenetic Dysregulation. Plos Biol. 2007; 5:e201. [PubMed: 17676974]

25. Valente G, et al. Distribution of interferon-gamma receptor in human tissues. Eur J Immunol. 1992; 22:2403–12. [PubMed: 1387613]
26. Feng C, et al. Mice deficient in LRG-47 display increased susceptibility to mycobacterial infection associated with the induction of lymphopenia. J Immunol. 2004; 172:1163–8. [PubMed: 14707092]
27. Der SD, Zhou A, Williams BR, Silverman RH. Identification of genes differentially regulated by interferon alpha, beta, or gamma using oligonucleotide arrays. Proc Natl Acad Sci USA. 1998; 95:15623–8. [PubMed: 9861020]
28. Essers M, et al. IFNα activates dormant haematopoietic stem cells in vivo. Nature. 2009:6.
29. Durbin JE, Hackenmiller R, Simon MC, Levy DE. Targeted disruption of the mouse Stat1 gene results in compromised innate immunity to viral disease. Cell. 1996; 84:443–50. [PubMed: 8608598]
30. Souroullas GP, Salmon JM, Sablitzky F, Curtis DJ, Goodell MA. Adult hematopoietic stem cell and progenitor cells require either Lyl1 or Scl for survival. Cell Stem Cell. 2009; 4:180–6. [PubMed: 19200805]
31. Durbin JE, Hackenmiller R, Simon MC, Levy DE. Targeted disruption of the mouse Stat1 gene results in compromised innate immunity to viral disease. Cell. 1996; 84:443–50. [PubMed: 8608598]
32. Muller U, et al. Functional role of type I and type II interferons in antiviral defense. Science. 1994; 264:1918–21. [PubMed: 8009221]
33. Feng C. The p47 GTPase Lrg-47 (Irgm1) Links Host Defense and Hematopoietic Stem Cell Proliferation. Cell Stem Cell. 2008; 2:83–89. [PubMed: 18371424]
34. Challen GA, Boles N, Lin KK, Goodell M. Mouse hematopoietic stem cell identification and analysis. Cytometry A. 2009; 75:14–24. [PubMed: 19023891]
35. Weksberg DC, Chambers SM, Boles NC, Goodell MA. CD150− side population cells represent a functionally distinct population of long-term hematopoietic stem cells. Blood. 2008; 111:2444–51. [PubMed: 18055867]
36. Souroullas GP, Salmon JM, Sablitzky F, Curtis DJ, Goodell MA. Adult hematopoietic stem cell and progenitor cells require either Lyl1 or Scl for survival. Cell Stem Cell. 2009; 4:180–6. [PubMed: 19200805]

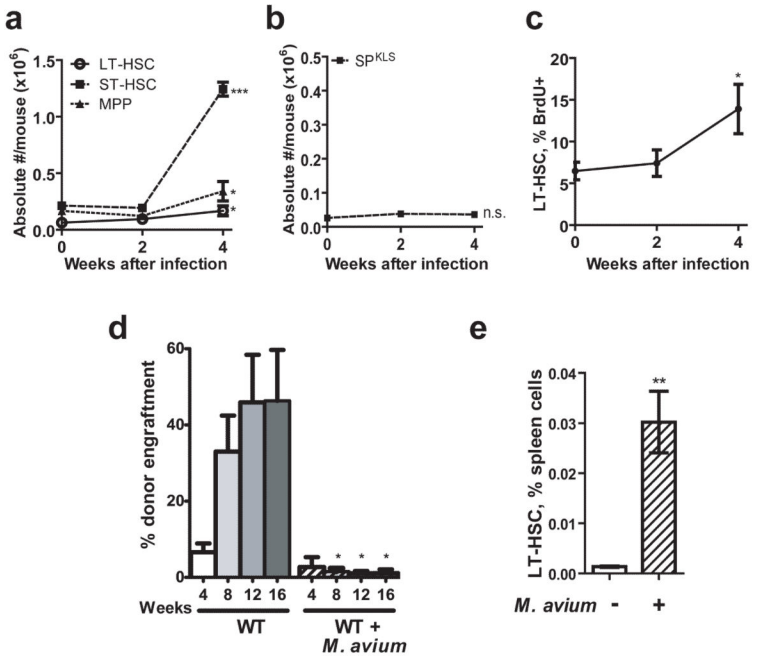

Figure 1.

Infection with *Mycobacterium avium* induces changes in hematopoietic stem cells. (A) Absolute numbers of short-term HSCs (ST-HSCs), multipotent progenitors (MPPs), and long-term HSCs (KSL, Flk2−, CD34−) were determined after infection with *M. avium*. n=3-7. (B) LT-HSCs (side population, lineage-negative, Sca-1+, c-Kit+ (SP^{KLS})) were not significantly changed after infection with *M. avium*. Plot is representative of three independent experiments, each with n=3-5. (C) BrdU incorporation in SP^{KLS} cells was determined at baseline and after infection. Data represent two independent experiments, each with n=2-5. (D) Engraftment efficiency was determined after transplantation of 500 SP^{KLS} from WT or *M. avium*-infected WT mice into lethally irradiated WT recipients. Data represent two independent experiments, each with n=2 to 6. (E) The percentage of LT-HSCs (KSL CD150+) in the spleen was determined at baseline and 4 weeks after *M. avium* infection. n=4 or 5.

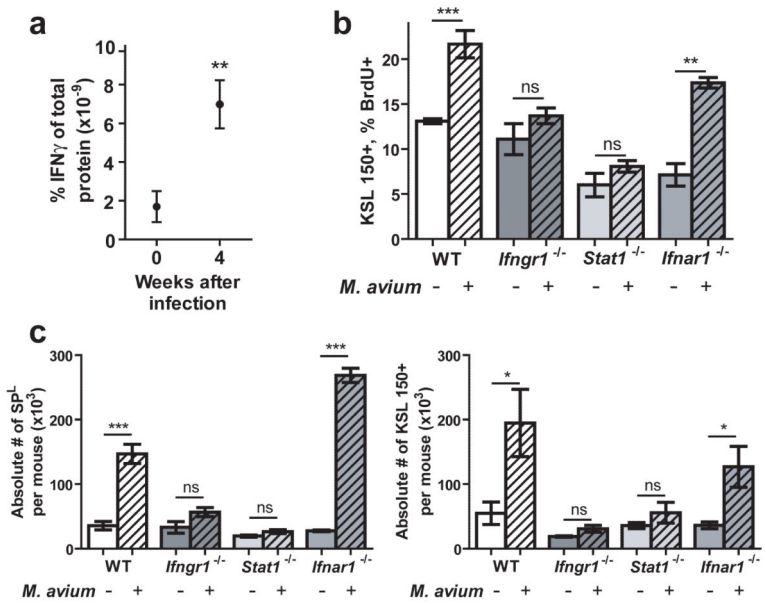

Figure 2.

The HSC response to *M. avium* infection is dependent upon intact IFNγ signaling.

(A) IFNγ levels in bone marrow supernatant were quantified by cytokine bead array at baseline and 4 weeks postinfection with *M. avium*. n=3-6. (B) BrdU incorporation by HSCs (KSL CD150+) of naïve and *M. avium*-infected WT, *Ifngr1*-deficient, *Stat1*-deficient, and *Ifnar1*-deficient mice was quantified. n=3-6. (C) Absolute number of HSCs (KSL CD150+) in the whole bone marrow of naïve and infected WT, *Ifngr1*-deficient, *Stat1*-deficient, and *Ifnar1*-deficient mice was determined. n=3-7.

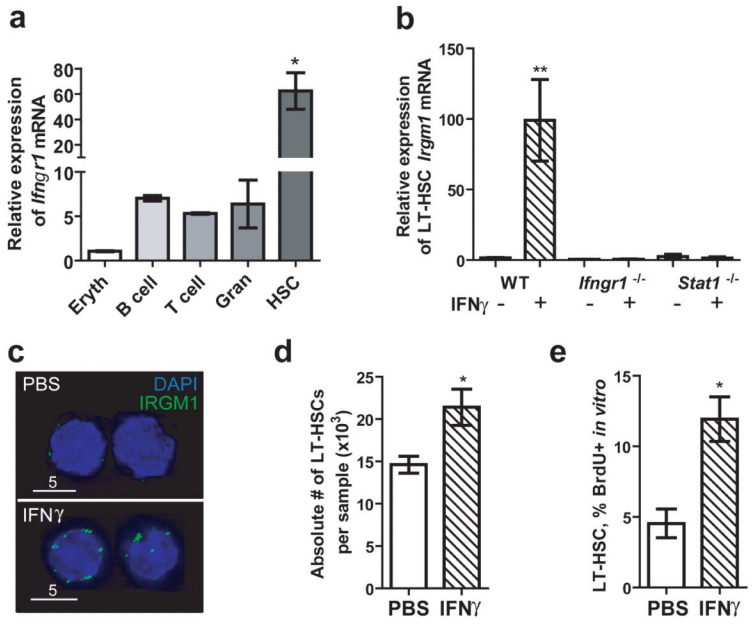

Figure 3.

IFNγ is sufficient to induce HSC proliferation *in vitro*.

(A) Relative quantities of *Ifngr1* mRNA were determined in pooled samples of nucleated erythrocyte progenitors ("Eryth"), B-cells, T-cells, granulocytes ("Gran"), and LT-HSCs (SP^{KLS}). n=2-3 independent samples per cell type. (B) *Irgm1* mRNA was quantified by real-time PCR in LT-HSCs (SP^{KLS}) after IFNγ treatment. (C) IRGM1 protein levels on LT-HSCs (SP^{KLS}) were determined by immunofluorescence. (D) BrdU incorporation by primitive hematopoietic cells (KSL CD150+) was assessed after 12-hour *in vitro* treatment with PBS or IFNγ. Data represent two independent experiments each performed in triplicate.

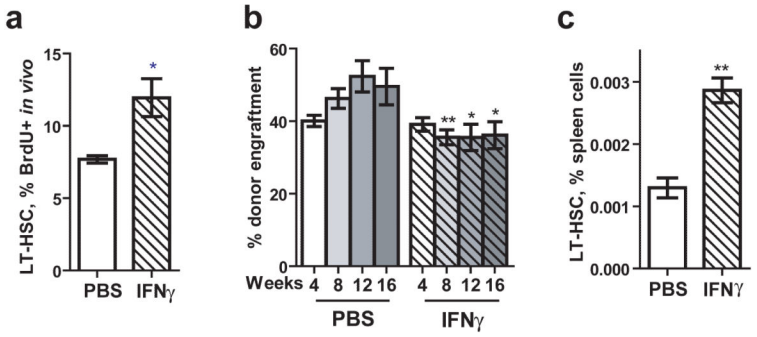

Figure 4.

IFNγ is sufficient to induce HSC proliferation *in vivo*.

(A) BrdU incorporation was measured in LT-HSCs (SP^{KLS}) of WT mice 24 hours after injection with IFNγ or PBS and 12 hours after injection with BrdU. n=5. (B) Whole bone marrow was isolated from PBS or IFNγ-injected WT mice 24 hours postinjection, and transplanted into lethally irradiated WT recipients in competitive transplant assays. Engraftment efficiency was determined 4, 8, 12, and 16 weeks after transplantation. n=5-6. (C) The percentage of primitive hematopoietic cells (KSL CD150+) in the spleen was determined 24 hours after injection with either PBS or IFNγ. n=3.

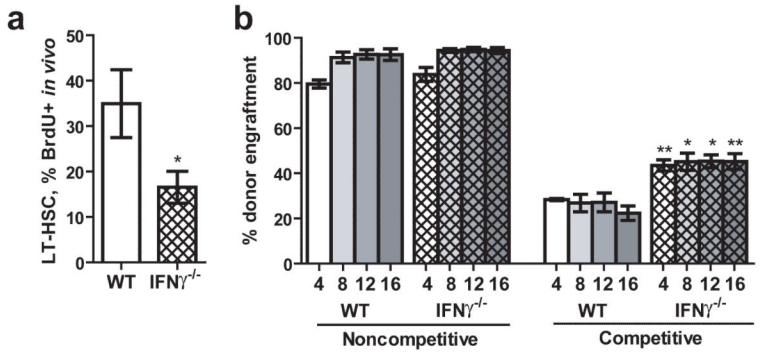

Figure 5.

Basal IFNγ tone affects HSC cycling and function.

(A) BrdU incorporation by LT-HSCs (SP^{KLS}) of WT and *Ifng*-deficient mice over 3 days was determined. n=4 or 5. (B) Engraftment efficiency was determined 4, 8, 12, and 16 weeks after transplantation of whole bone marrow from WT or *Ifng*-deficient mice into lethally irradiated WT recipients in either noncompetitive or competitive transplant assays. n=5.